

# We are IntechOpen, the world's leading publisher of Open Access books Built by scientists, for scientists

**4,800**

Open access books available

**122,000**

International authors and editors

**135M**

Downloads

Our authors are among the

**154**

Countries delivered to

**TOP 1%**

most cited scientists

**12.2%**

Contributors from top 500 universities



**WEB OF SCIENCE™**

Selection of our books indexed in the Book Citation Index  
in Web of Science™ Core Collection (BKCI)

Interested in publishing with us?  
Contact [book.department@intechopen.com](mailto:book.department@intechopen.com)

Numbers displayed above are based on latest data collected.

For more information visit [www.intechopen.com](http://www.intechopen.com)



# Determination of the Local Crystal-Chemical Features of Complex Chalcogenides by Copper, Antimony, and Arsenic NQR

R.R. Gainov<sup>1,2</sup>, A.V. Dooglav<sup>1</sup>, I.N. Pen'kov<sup>2</sup>, A.Yu. Orlova<sup>1</sup>,  
I.A. Evlampiev<sup>1</sup>, N.N. Mozgova<sup>3</sup>, and R.R. Khasanov<sup>2</sup>

<sup>1</sup>*Department of Physics, Kazan Federal University, Kazan, Kremlevskaya str. 18, 420008,*

<sup>2</sup>*Department of Geology, Kazan Federal University, Kazan, Kremlevskaya str. 4/5, 420111,*

<sup>3</sup>*Institute of geology of ore deposits, petrography, mineralogy and geochemistry of the Russian Academy of Science, Staromonetny per. 35, Moscow 109017,*

*Russian Federation*

## 1. Introduction

In recent years, a number of reviews have appeared in scientific literature on the application of different physical methods in the structural-chemical and physical studies of solid state materials, for example, high-temperature superconductors (HTSC). An important place among them is occupied by nuclear-resonance methods, particular, nuclear magnetic resonance (NMR), nuclear quadrupole resonance (NQR), nuclear gamma resonance (NGR or Mössbauer spectroscopy) and other. Particularly, this article shows the feasibility of using the NQR method, in some instance, in the study of those features of material structure and chemistry, which are difficult or impossible to attack by conventional methods. The key advantage of NQR is a possibility to probe directly the electric (quadrupole) interactions between nuclei and their local environment. In general, the quadrupole interaction describes the coupling of the nuclear quadrupole moment to the electric field gradient (EFG). The EFG is determined by bond directions and electronic charge distribution, therefore the quadrupole interaction is a very sensitive tool for structural-chemical studies of condensed matter. Notably, it is possible to analyze NQR data (both the spectroscopic and the relaxation) in materials containing different structural copper (<sup>63,65</sup>Cu), arsenic (<sup>75</sup>As), and antimony (<sup>121,123</sup>Sb) complexes. This circumstance is especially important in the light of existence of two types of HTSC: Cu-oxide materials (cuprates) (Rigamonti et al., 1998) and As- and Sb-bearing pnictides (Wilson, 2009).

Our article is devoted to brief review of some important spectroscopic experimental results obtained during the studies of binary chalcogenide CuS (also known as covellite), representing the unusual low-temperature superconductor, and ternary material Ag<sub>5</sub>SbS<sub>4</sub> (referred to as a stephanite). Examples are taken mainly from the studies of the authors' research group.

The article is organized as follows. Section I contains necessary NQR background for <sup>63,65</sup>Cu, <sup>75</sup>As, <sup>121,123</sup>Sb nuclei. In Section II we report our results concerning the covellite CuS and

some related materials with subsequent discussions. Section III is devoted to studies of stephanite  $\text{Ag}_5\text{SbS}_4$  in connection with other related compounds. The paper concludes with a summary in Section IV.

## 2. NQR background

The NQR background will be reviewed only for the sake of clarity (Grechishkin, 1973). The nuclear spins  $I$  interact with their electronic environment through quadrupole (i.e. electric) and magnetic hyperfine couplings. In general, the NQR spectrum is described by the following Hamiltonian:

$$H_Q = \frac{eQV_{ZZ}}{4I(2I-1)} \left\{ 3I_Z^2 - I(I+1) + \frac{1}{2}\eta(I_+^2 + I_-^2) \right\} \quad (1)$$

Hamiltonian  $H_Q$  refers to as the coupling of nuclear quadrupole moment  $eQ$  to the local crystal electric field gradient (EFG) with  $V_{ZZ}$  the largest component of the crystal EFG tensor,  $\eta = |V_{XX} - V_{YY}|/V_{ZZ}$  the asymmetry parameter showing the deviation of the EFG symmetry from the axial one, i.e. the value of  $\eta$  lies in the range  $[0,1]$ . The EFG components satisfy Laplace equation:  $V_{XX} + V_{YY} + V_{ZZ} = 0$ .

The pure NQR spectrum is observed in the case of absence of the external ( $H_0=0$ ) and internal ( $H_{int}=0$ ) static magnetic fields. The number of NQR lines is defined (i) by the amount of crystallographically nonequivalent positions of quadrupole nucleus ( $I > 1/2$ ) in the crystal structure, (ii) by the local geometry (i.e. symmetry) of quadrupole nucleus surrounding, (iii) by the magnitude of nuclear spin  $I$  and (iv) by the number of naturally available isotopes of quadrupole nucleus.

In case of copper, only two naturally available isotopes exist:  $^{63}\text{Cu}$  (69.2% natural abundance,  $\gamma/2\pi=1.128$  kHz/Oe,  $Q=-0.22$  barn) and  $^{65}\text{Cu}$  (30.8% natural abundance,  $\gamma/2\pi=1.209$  kHz/Oe,  $Q=-0.204$  barn) both having spin  $I=3/2$  and thus two doubly degenerate  $\pm 1/2$  and  $\pm 3/2$  energy levels. Thus, for each isotope a transition between these levels yields a single NQR signal at a frequency:

$${}^{63,65}v_Q = \frac{e \cdot {}^{63,65}QV_{ZZ}}{2h} \cdot \sqrt{1 + \frac{1}{3}\eta^2}. \quad (2)$$

Arsenic has a single total-lot isotope  $^{75}\text{As}$  ( $I = 3/2$ , 100% natural abundance,  $\gamma/2\pi=0.729$  kHz/Oe,  $Q=0.3$  barn), therefore the single arsenic crystal-chemical position gives only one NQR signal at a frequency:

$${}^{75}v_Q = \frac{e \cdot {}^{75}QV_{ZZ}}{2h} \cdot \sqrt{1 + \frac{1}{3}\eta^2}. \quad (3)$$

Antimony has two naturally occurring isotopes  $^{121}\text{Sb}$  ( $I = 5/2$ , 57.3% natural abundance,  $\gamma/2\pi=10,188$  MHz/T,  $Q=-1.3$  barn) and  $^{123}\text{Sb}$  ( $I = 7/2$ , 45.7% natural abundance,  $\gamma/2\pi=5,517$  MHz/T,  $Q=-0.18$  barn). The  $^{121}\text{Sb}$  exhibits two NQR signals at frequencies ( $\eta < 0.2$ ):

$${}^{121}v_{Q(\pm 3/2 \leftrightarrow \pm 1/2)} = \frac{3e \cdot {}^{121}QV_{ZZ}}{20h} \cdot \left(1 + \frac{59}{54} \cdot \eta^2\right), \quad (4a)$$

$${}^{121}\nu_{Q(\pm 5/2 \leftrightarrow \pm 3/2)} = \frac{6e \cdot {}^{121}QV_{ZZ}}{20h} \cdot \left(1 - \frac{11}{54} \cdot \eta^2\right). \quad (4b)$$

The  ${}^{123}\text{Sb}$  with  $I=7/2$  has three NQR signals at frequencies ( $\eta < 0.2$ ):

$${}^{123}\nu_{Q(\pm 3/2 \leftrightarrow \pm 1/2)} = \frac{e \cdot {}^{123}QV_{ZZ}}{14h} \cdot \left(1 + \frac{109}{30} \cdot \eta^2\right), \quad (4c)$$

$${}^{123}\nu_{Q(\pm 5/2 \leftrightarrow \pm 3/2)} = \frac{2e \cdot {}^{121}QV_{ZZ}}{14h} \cdot \left(1 - \frac{17}{30} \cdot \eta^2\right), \quad (4d)$$

$${}^{123}\nu_{Q(\pm 7/2 \leftrightarrow \pm 5/2)} = \frac{3e \cdot {}^{121}QV_{ZZ}}{14h} \cdot \left(1 - \frac{1}{10} \cdot \eta^2\right). \quad (4e)$$

Thus, the single antimony crystal-chemical position in the structure of material under study yields five NQR signals.

As one can see, NQR frequency  $\nu_Q$  depends on the certain arrangement of the surrounding ions through the parameters  $V_{ZZ}$  and  $\eta$ . The value of  $\nu_Q$  is defined by two parameters in Eq.(4):  $V_{ZZ}$  and  $\eta$ ; so it is impossible to obtain both parameters experimentally from the NQR spectra consisting of only one line for  $I=3/2$  (copper and arsenic). Usually it is done from the angular dependence of the NMR spectrum taken for a single crystal or from numerical simulations of NMR spectrum for the unaligned powder. In some cases, for determination of  $\eta$  the 2D nutation NQR studies also could help.

In a semi-empirical approach (Kaufmann & Vianden, 1979), it is assumed that components of EFG tensor at Cu nuclei site can be written as the sum of two terms – lattice and valence contributions:

$$V_{ZZ} = (1 - \gamma_{\infty}) \cdot V_{latt} + (1 - R_{val}) \cdot V_{val} \quad (5)$$

The parameters  $\gamma_{\infty}$ ,  $R_{val}$  are the Sternheimer antishielding factors. The first contribution arises from all ion charges outside the ion under consideration and can be calculated using the model of point-charges (MPC):

$$V_{latt} = \sum_i \frac{q_i \cdot (3 \cdot \cos^2 \theta_i - 1)}{r_i^3}, \quad (6)$$

where  $q_i$  and  $r_i$  are the charge and the position of the  $i$ -th ion, respectively,  $\theta_i$  – angle between main axis of symmetry and direction into the neighboring ion.

The computation of valence contribution  $V_{val}$  (and, as consequence, total  $V_{ZZ}$ ) constitutes a complex problem, since it requires a detailed knowledge of the structure and electronic density distribution. On the other hand, the comparison of  $\nu_Q$  and  $V_{ZZ}$ , deduced from theoretical calculations on the basis of different structural models and approaches (see Eq.(5)), with experimental values (Eq.(4)) permits to determine the individual features of local electronic arrangement and peculiarities of chemical bonds. Actually, the lattice contribution  $V_{latt}$  is defined by crystal symmetry, whereas the valence contribution  $V_{val}$  is determined by the local symmetry of nearest environment, i.e. according to NQR frequencies and line-widths it is possible to investigate the following EFG characteristics: the

electronic density distribution inside of different coordination complexes and their symmetry, the extent of ionic (covalent) bonds and angles between them. Every factor, which is connected with reorganization of atomic or molecular group, can change significantly the EFG value on the nucleus inside of a such group and, as consequence, NQR is very sensitive to different crystal-chemical transformations in crystal lattice. Therefore, the studies of temperature dependences of NQR spectroscopic parameters give the possibility to find phase transitions and investigate their nature.

### 3. Towards to electronic structure of binary copper chalcogenides

There is a great number of compounds in the system of binary copper chalcogenides Cu-S, Cu-Se, and Cu-Te. In particular, materials eleven natural minerals and two unstable synthetic phases among only binary copper-sulfide have been discovered up to date (Goble, 1985; Gablina, 1997). Many of them are widely used in optoelectronics (Abrikosov et al., 1975; Isac et al., 2007) and some of them represent the industrial mineral specimens in copper-ore deposits (Izoitko, 1997). The more significant involving of these compounds into the practical application is stopped by the fact that currently available standard instrumental techniques for studying crystal-chemical problems such as X-ray structural diagnosis, optical spectroscopy, and electronic microscopy have inherent limitations (Gablina, 1997). These manifest themselves in being unable to characterize the chalcogenides samples fully, especially if they are polycrystalline. These methods are mainly ineffective and little informative in case of multiphase natural samples (minerals) (Gablina, 1997).

This Section describes briefly the spectroscopic studies of layered low-temperature superconductor CuS (covellite, originally published in (Gainov et al., 2009)) and related, potentially perspective, but insufficiently known compounds: non-stoichiometric sulfide  $\text{Cu}_{1.6}\text{S}$  (naturally occurring as geerite) and selenium analog of CuS –  $\alpha\text{-CuSe}$  (klockmannite). The description of experimental methodic and synthesis conditions can be found in (Gainov et al., 2009).

#### 3.1 Crystal-chemistry of CuS, $\text{Cu}_{1.6}\text{S}$ , and $\alpha\text{-CuSe}$

Covellite CuS represents the metal with excellent hole conductivity, which becomes anisotropically superconducting below  $T_C = 1.6$  K (Meissner, 1929; Buckel & Hilsch, 1950; Saito et al., 1997; Di Benedetto et al., 2006). The elementary cell of CuS at room- $T$  has a hexagonal symmetry (space group  $P6_3/mmc$ ) (Berry, 1954; Evans & Konnert, 1976; Ohmasa et al., 1977). The structure of CuS can be described as a “sandwich”, which consists of three alternating layers  $A_1$ -B- $A_2$  (Fig. 1). The layer B represents the net of  $[\text{Cu}(1)\text{-S}(1)_3]$ -triangles, whereas the layers  $A_1$  and  $A_2$  are made up of  $[\text{Cu}(2)\text{-S}(1)\text{S}(2)_3]$ -tetrahedra. The units  $A_1$ -B- $A_2$  are connected together along the  $c$ -axis by S(2)-S(2) bonds. It was revealed that the second-order phase transition (PT) is occurred at about  $T_{PT} = 55$  K (Fjellvåg et al., 1988). This transition can be presented as a little shift of the layer B with respect to the layers  $A_1$  and  $A_2$  perpendicular to the  $c$ -axis with the change of the Cu(2)-S(1)-Cu(2) bonding angle from  $180^\circ$  at room- $T$  to  $170^\circ$  below  $T_{PT}$ .

The crystal structure of klockmannite  $\alpha\text{-CuSe}$  is not identified in detail up to date. As a first approach, it is assumed that the structure of  $\alpha\text{-CuSe}$  is somewhat similar to those in CuS (Berry, 1954; Peiris et al., 1998; Milman, 2002): there are the same space group and layered motive  $A_1$ -B- $A_2$  with the  $\text{CuSe}_3$ ,  $\text{CuSe}_4$ , and Se-Se complexes. At the same time, it is proposed the occurrence of CuS-based superlattice in klockmannite (Berry, 1954).

The structure of geerite  $\text{Cu}_{1.6}\text{S}$  is unsolved. It was suggested only that  $\text{Cu}_{1.6}\text{S}$  can have a structure with the blende-like subcell (Goble, 1985).

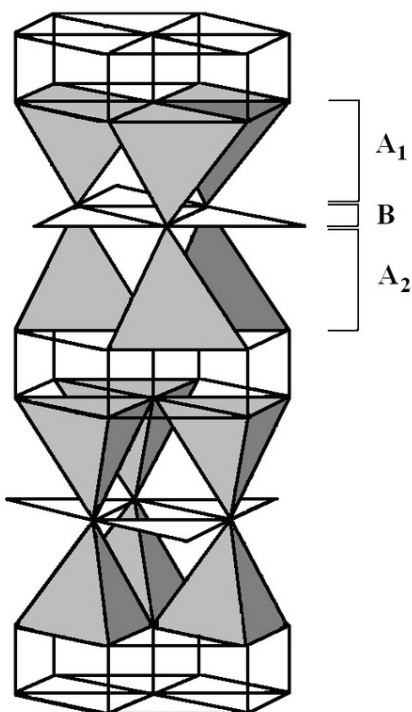


Fig. 1. Crystal structure of the covellite  $\text{CuS}$  above  $T_{PT} = 55$  K. For details, see text

### 3.2 NQR spectra of $\text{CuS}$ , $\text{Cu}_{1.6}\text{S}$ , $\alpha\text{-CuSe}$

In Table I the NQR frequencies observed for the title materials together with previously published data are listed. As one can see, the values of NQR frequencies are quite different. However, their comparison and analysis can allow us to reveal some unique features of compounds studied.

Let us start from the covellite  $\text{CuS}$ . It was found that copper NQR spectra of both synthetic and natural samples of  $\text{CuS}$  contain two copper pairs (Gainov et al., 2009). The presence of two spectral pairs permits us to assert that NQR spectra reflect the occurrence of two crystallographically non-equivalent sites of copper nuclei in  $\text{CuS}$ . The first pair, attributed to three-coordinated  $\text{Cu}(1)$ , is placed at 14.88 ( $^{63}\text{Cu}$ , 4.2 K) and 13.77 MHz ( $^{65}\text{Cu}$ , 4.2 K) (Fig. 2(a)), whereas the second pair, assigned to four-coordinated  $\text{Cu}(2)$  site (not shown here, see (Gainov et al., 2009)), is located at 1.87 ( $^{63}\text{Cu}$ , 4.2 K) and 1.73 MHz ( $^{65}\text{Cu}$ , 4.2 K). In general, there is no EFG at the sites with cubic local symmetry (Slichter, 1996). This case is taken place for the tetrahedral  $\text{Cu}(2)$  sites in layers  $A_1$  and  $A_2$  (Fig. 1). However, significant deformations of the  $\text{CuS}_4$  tetrahedrons break the cubic symmetry and, as consequence, EFG on the copper nucleus in this position becomes nonzero. The appearance of low-frequency NQR signals points that this case is realized actually for the tetrahedral  $\text{Cu}(2)$  sites in  $\text{CuS}$ . Therefore, our NQR spectra prove strongly the crystallographic data (Fjellvåg et al., 1988) concerning the occurrence of low-symmetry distortions around  $\text{Cu}(2)$  sites below  $T_{PT} = 55$  K. Other words, NQR spectra can serve as an independent confirmation of the low- $T$  model of the  $\text{CuS}$  structure.



Material	Positions	<sup>63</sup> Cu NQR frequencies <sup>1</sup> , MHz (T = 4.2 K)
CuS (covellite)	Site 1	14.89
	Site 2	1.87
Cu <sub>1.6</sub> S (geerite)	Site 1	16.95
	Site 2	16.20
	Site 3	15.25
	Site 4	11.95
	Site ?	Below 2 MHz?
α-CuSe (klockmannite)	Site 1	12.17
	Site 2	11.89
	Site 3	9.49
	Site 4	9.39
	Site 5	8.27
	Site 6	6.60
	Site 7	6.50
	Site 8	4.49
	Site 9	4.01
	Site 10	3.75
	Site 11	3.29
	Site 12	2.83
	Site 13	2.09

<sup>1</sup> The values of NQR frequencies for <sup>65</sup>Cu isotope can be calculated in accordance with ratio  $\nu_Q(^{63}\text{Cu})/\nu_Q(^{65}\text{Cu}) = 1,081$ .

Table I. NQR frequencies for CuS and some related compounds.

High-frequency NQR spectra, corresponding to triangular Cu(1), are also intriguing (Fig. 2(a)). It is notable that these NQR signals are placed at lower frequency range in comparison with the region of 20-25 MHz, in frame of which NQR signals of majority of other copper sulfides lie (Abdullin et al., 1987). In case of copper sulfides EFG is mainly formed by the lattice term and a quite narrow range of the  $\nu_Q$  changes can be explained by insignificant variations of the Cu-S distances, S-Cu-S angles and the polarity of chemical bonds. In fact, such conclusion was checked by theoretical calculations according to Mulliken-Wolfsberg-Helmholtz method (Abdullin et al., 1987). This result indicates directly that the valence contribution for the EFG at the Cu(1) site in CuS is more considerable than in case of triangular units CuS<sub>3</sub> of other sulfides. Analysis shows that the more probable reason of this unusual  $\nu_Q$  lowering is connected with anomalously short Cu(1)-S distances in CuS (2.19 Å) compared to those in other sulfides ( $\approx 2.33$  Å). It seems, however, that due to Bayer's influence of thermal-induced lattice vibrations, NQR frequency  $\nu_Q$  must increase with decreasing distances as it takes place in most compounds (Semin et al., 1975): according to MPC model (Eq.(6)), EFG is inversely proportional to the distance between metal and ligand. On the other hand, the shortening of metal-ligand distances can lead to charge transfer with subsequent redistribution on the different orbitals (Semin et al., 1975). In our case this process can be related to the charge transfer between valency Cu-4p,3d and S-3p orbitals (Gainov et al., 2009). Indeed, in frame of the semi-empirical approach (Section I), the valence contribution to the EFG,  $V_{val}$ , is related particularly to the various electronic hole densities as follows:

$$V_{val}^{(4p)} = A \cdot \langle r^{-3} \rangle_{4p} \cdot [N_{4p(z)} - \frac{1}{2}N_{4p(x)} - \frac{1}{2}N_{4p(y)}], \quad (7)$$

where  $A$  is a constant,  $N_{3d(x,y,z)}$  and  $N_{4p(x,y,z)}$  are the numbers of electronic holes in different Cu-4p orbitals, the charge of an electron is given by  $-e$ . In this way, the hole concentration can be estimated from the change of  $\nu_Q$ . It was pointed that the shortening of Cu-S distances in Cu(1)S<sub>3</sub> complexes in CuS can lead to decreasing electronic density of the Cu-4p<sub>z</sub> orbital and increasing population of Cu-4p<sub>x</sub> and Cu-4p<sub>y</sub> orbitals. According to Eq.(7) this factor can play a vital role in the lowering of the total EFG value at the Cu site by about 5 MHz. Thus, the experimentally observed shift of the high-frequency <sup>63</sup>Cu(1) NQR signal from the frequency range of 20–25 MHz typical for three-coordinated Cu by S atoms in other copper sulfides can serve as an indication of the strong hybridization of Cu(1)–S chemical bonds in Cu(1)S<sub>3</sub> complexes. Remarkably, this conclusion was confirmed later by studies of copper nuclear spin-lattice relaxation (Gainov et al., 2009).

Let us compare now the <sup>63</sup>Cu NQR spectra of covellite CuS and geerite Cu<sub>1.60</sub>S (Fig. 2(b)-2(d), Table I). As one can see, the samples studied are multiphase and contain two structural phases (CuS and Cu<sub>1.60</sub>S).

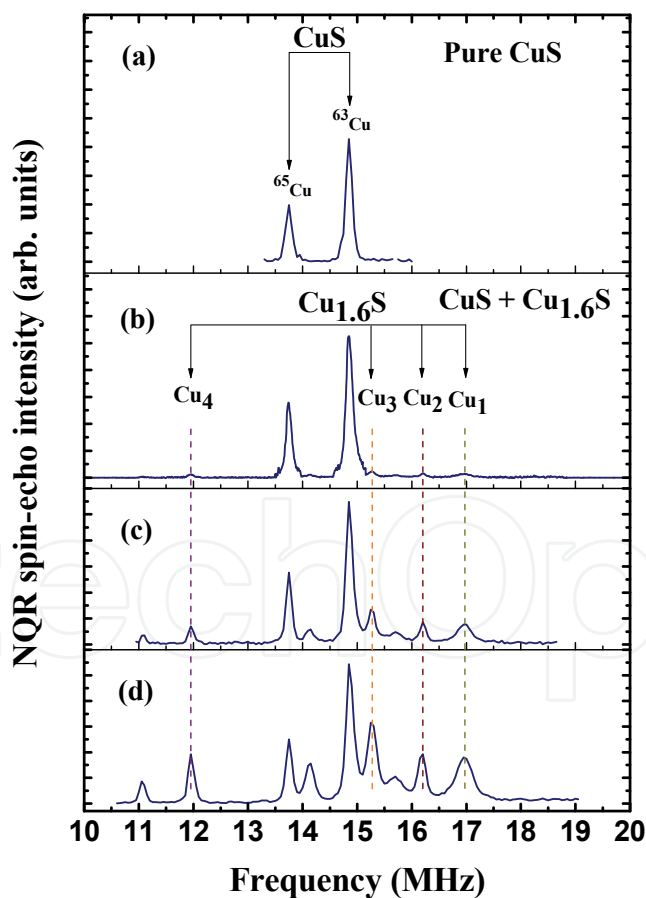


Fig. 2. High-frequency copper NQR spectra for covellite, CuS, and geerite, Cu<sub>1.6</sub>S. Arrows point to the positions of <sup>63,65</sup>Cu(1) NQR signals of CuS. The vertical dashed lines point to the positions of <sup>63</sup>Cu NQR signals of Cu<sub>1.6</sub>S phase For details, see text.



The principle difference between samples is a variation of quantitative proportion of CuS and Cu<sub>1.60</sub>S. The NQR spectra of such samples are convenient for detailed discussion. As indicated in Fig. 2, at high-frequency range (10.00-17.00 MHz) there are five copper NQR pairs, one of them corresponds to covellite CuS (exact coincidence of Cu line frequencies); the additional four Cu pairs belong to another structural phase – geerite Cu<sub>1.60</sub>S. Notably, the NQR spectra, which pertain to this phase, coincide in all multiphase samples and include the following lines: 16.95, 16.20, 15.25, 11.95 MHz for <sup>63</sup>Cu and 15.67, 14.98, 14.11, 11.06 MHz for <sup>65</sup>Cu. It should be noted that our results prove fully the previous data for Cu<sub>1.6</sub>S (Anashkin et al., 1994), according to which these eight Cu NQR lines have been observed at the same frequencies. It is interesting that the NQR signal intensities of Cu<sub>1.6</sub>S phase increase with increasing amount of Cu<sub>1.6</sub>S and, simultaneously, the signals intensities of CuS decrease according to the same proportion (Fig. 2). We note here that this fact can in general serve as supplementary striking evidence for the possibility to use NQR method in qualitative and quantitative phase-analytical diagnostics of different chalcogenides.

As it was pointed above (Section I), the number of NQR centers in the structure of material studied is not less than the amount of crystallographically non-equivalent positions of resonant nuclei. At least four centers exist in case of geerite Cu<sub>1.6</sub>S (four pairs of <sup>63</sup>Cu and <sup>65</sup>Cu lines). Hence, the total number of different crystal-chemical sites of copper in this compound is not less than four. This circumstance reflects the serious distinction in symmetry of CuS and Cu<sub>1.6</sub>S electronic structures. On the other hand, we can see that the range of 10.00-17.00 MHz, in frame of which eight <sup>63,65</sup>Cu lines of Cu<sub>1.6</sub>S are located, is also not typical for NQR signals exhibited by most of copper sulfides. Moreover, NQR lines of Cu<sub>1.6</sub>S are grouped around the high-frequency Cu NQR signal of covellite CuS. Taking into account these two aspects, it is possible to claim that the electronic structures of CuS and Cu<sub>1.60</sub>S are still different, but they have the same crystal-chemical motive. In principle, our NQR results suggest that the structure Cu<sub>1.60</sub>S can be interpreted as the derivative of covellite CuS structure with the strong deformations. To our knowledge, this conclusion is a first experimental argument in favor of crystallographical proximity between CuS and Cu<sub>1.60</sub>S phases.

We turn now to the <sup>63</sup>Cu NQR spectrum for CuS and the <sup>63</sup>Cu NQR spectrum for selenium analog of CuS – klockmannite, α-CuSe (Table I). Their comparative analysis can also introduce new information concerning their electronic structure as well as highlight some reasons for low-temperature phase transitions in these materials (Section II.1). In general, the copper selenide CuSe undergoes two phase transitions upon cooling: from γ-CuSe into β-CuSe modification near 398 K and to α-CuSe at 323 K (Nozaki et al., 1995; Milman, 2002). It was proposed that α-CuSe has the same structure as CuS (Berry, 1954) and the β-γ transformation of CuSe is similar to that in CuS at  $T_{PT}=55$  K (Nozaki et al., 1995). Notably, Raman spectroscopy and powder X-ray diffractometry shows that in the system of CuS<sub>1-x</sub>Se<sub>x</sub> (0 ≤ x ≤ 1) compounds  $T_{PT}$  increases from 55 K for x=0 up to 398 K for x=1 (Nozaki et al., 1995). However, it was found that α-CuSe is characterized by 13 lines in the spectrum with NQR frequencies in the range of 13–2 MHz at 4.2 K. First, this aspect points strongly to the presence of strong deformations of the α-CuSe crystal and gives evidence that CuS and α-CuSe are not isostructural as it was supposed earlier (Berry, 1954). It is clearly seen that α-CuSe has at least 13 non-equivalent Cu positions. These data point that α-CuSe can be considered as distorted version of CuS-based structure. Second, <sup>63</sup>Cu NQR frequencies in α-CuSe are rather low as compared with that in CuS. This indicates that insertion of Se atoms

instead of S in CuS results in the conversion of Cu(1) threefold units (Fig. 1) into distorted fourfold ones in  $\text{CuS}_{1-x}\text{Se}_x$ . However, such a substitution mechanism implies basically the preservation of layered structural motive in  $\text{CuS}_{1-x}\text{Se}_x$  (as in CuS). The preferential occupation of Se at the S(2) sites (Nozaki et al., 1995) leads to the approaching of some Se(2) atoms to Cu(1) sites and to the formation of distorted tetrahedrons  $\text{Cu(1)Se(1)}_3\text{Se(2)}_1$  in  $\alpha$ -CuSe instead of triangular units  $\text{Cu(1)S(1)}_3$  in CuS (Fig. 1). In this case such deformations would promote the approaching of Cu(1) and Cu(2) ions to each other and creation of an effective interaction between them, as it was proposed for CuS and  $\alpha$ -CuSe earlier (Fjellvåg et al., 1988; Milman, 2002). Upon cooling this interaction can stimulate the phase transition. Such scenario is supported by the dependence of the  $T_{PT}$  value on the Se amount in mixed samples  $\text{CuS}_{1-x}\text{Se}_x$  ( $0 \leq x \leq 1$ ) (Nozaki et al., 1995). Actually, since the Cu(1)-Cu(2) bonds in CuS are longer than that in  $\text{CuS}_{1-x}\text{Se}_x$ , this phase transition in CuS occurs at lower  $T$ . Thus, NQR spectra signify that  $\alpha$ -CuSe material is related crystal-chemically to CuS and have a somewhat similar layered structure, but either of  $\text{Cu(1)Se}_3$  and  $\text{Cu(2)Se}_4$  complexes in this compound are strongly distorted and this aspect leads again to layered  $A_1$ - $B$ - $A_2$  structure, as in CuS, but with different and uncertain structures of layers  $A_1$ ,  $A_2$ , and  $B$  (Fig. 1).

### 3.3 Temperature dependences of NQR spectra of CuS, $\text{Cu}_{1.6}\text{S}$ , $\alpha$ -CuSe

The dependence of the high-frequency  $^{63}\text{Cu(1)}$  NQR line of CuS on temperature is shown in Fig. 3. As one can see, the quadrupole frequency  $\nu_Q$  decreases with increasing temperature without significant anomalies. However, there exist two weak effects: the change of the slope in the temperature dependence of  $\nu_Q$  at 65 K (near  $T_{PT}$ ) and 210 K. In order to describe an approximate behavior of  $\nu_Q$  in the region of 65–290 K we applied the following equation (Kaufmann & Vianden, 1979):

$$\nu_Q(T) = \nu_Q(0) \cdot (1 - a \cdot T^b), \quad (8)$$

where  $\nu_Q(0)$ ,  $a$  and  $b$  are the fitting parameters. The best result of fitting depicted in Fig. 3 by solid curve was obtained for  $\nu_Q(0) = (14.95 \pm 0.02)$  MHz,  $a = (1.7 \pm 0.5) \cdot 10^{-4}$  MHz/K and  $b = (0.98 \pm 0.05)$ . It has been argued that the dependence of the NQR frequency in CuS on temperature can be understood in terms of charge fluctuations in Cu(1)-S(1)-Cu(2) bonds. It is known that a lot of non-cubic metals  $\nu_Q(T)$  can be well reproduced by the empirical Eq. (8) with  $b=1.5$ ; this relation is often referred to as the “ $T^{3/2}$  law” (Kaufmann & Vianden, 1979). No reliable explanation of the  $T^{3/2}$  temperature dependence of  $\nu_Q$  has been presented in the literature (Kaufmann & Vianden, 1979; Torumba et al., 2006). However, it is proposed that thermal vibrations of the host lattice atoms are regarded as responsible for such universal relation. CuS shows another relation – parameter  $b$  is close to 1 and, as consequence,  $\nu_Q(T)$  does not follow the  $T^{3/2}$  law. Such unusual behavior of  $\nu_Q$  is observed in mixed-valence metals, for example, in  $\text{EuCu}_2\text{Si}_2$  (Sampathkumaran, et al., 1979). The principle distinction of mixed-valence metals from “simple” ones is a variable number of conduction electrons (holes), which can “stick” temporary to ionic orbitals as valence electrons (holes). This valence instability initiated by Eu ions influences indirectly the Cu quadrupole interactions ( $V_{ZZ}$ ) and, as it was shown experimentally, the  $T^{3/2}$  law becomes not valid. Since in the range of 60–290 K there are no structural changes in CuS ( $\eta \approx 0$ ), the dependence of  $\nu_Q$  on temperature is determined only by  $V_{ZZ}$ . In a similar manner, the bridging S(1) ion in CuS can provide a minor charge transfer between Cu(1) and Cu(2) in some fluctuating regime. The strong hybridization of Cu(1) and Cu(2) conduction bands via S(1) atom, which was

revealed by means of analysis of NQR spectra and nuclear relaxation (Section II.2), should allow this transfer.

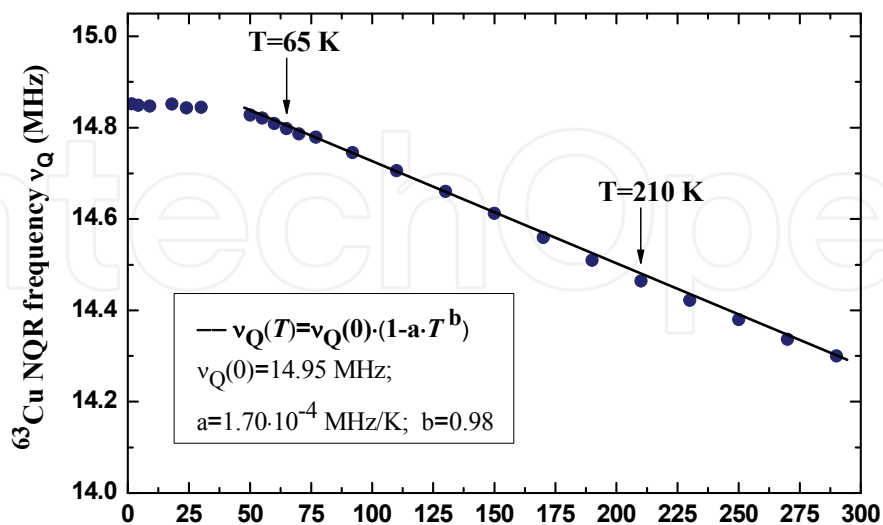


Fig. 3. The temperature dependence of  $^{63}\text{Cu}(1)$  NQR frequency for CuS (points) with the fit of data by Eq. (8) within 65–290 K (curve) and extracted fitting parameters. Arrows point to the positions of the change of slope in the  $\nu_Q(T)$  dependence at 210 K and at 65 K. For details, see text.

Remarkably that the temperature dependences of NQR frequencies in geerite  $\text{Cu}_{1.6}\text{S}$  (Section II.2) have the same linear character, as it takes place in case of covellite CuS (results will be published in forthcoming paper). This experimental feature can also serve as indication of the similarity of CuS and  $\text{Cu}_{1.6}\text{S}$  structures. Furthermore, the proximity of NQR spectra for CuS and  $\text{Cu}_{1.6}\text{S}$  materials and their analogous temperature dependences provide evidence that the main structural block of geerite was inherited from covellite CuS. The temperature dependences of some NQR frequencies in  $\alpha\text{-CuSe}$  were also monitored in the range of 4.2–77 K (Anashkin et al., 1994). It was found that the temperature gradient of NQR frequencies is rather small, although the dispersion of NQR frequencies is substantial. These data are also point that CuS and  $\alpha\text{-CuSe}$  have the similar features in lattice dynamics, where the layered structural motive and comparable coordination complexes play the essential role.

#### 4. Towards to electronic structure of antimony chalcogenides $\text{Sb}_2\text{S}_3$ , $\text{As}_5\text{SbS}_4$ , $\text{Ag}_3\text{SbS}_3$

The binary and ternary chalcogenide compounds of As, Sb, and Bi have the structures, which are closely related to zinc blende or wurtzite materials. As copper chalcogenides, some of them are used in optoelectronics (Abrikosov et al., 1975) and these compounds also represent the economically important minerals, which serve, for example, as sources of silver. From “scientific” position, these materials are interesting due to the fact that many of them undergo phase changes at low temperatures from ordered states to cation-disordered ones. The disordered states in these materials have potentially useful unique physical properties. For example, proustite  $\text{Ag}_3\text{AsS}_3$  and pyrargyrite  $\text{Ag}_3\text{SbS}_3$  appear to be excellent model crystals for studies of commensurate and incommensurate ferroelectric properties (Blinic & Zeks, 1974). Experience has proved that NQR in combination with X-ray analysis

can be as an effective tool for studies of detailed aspects of such phases (Blinic & Zeks, 1974). In spite of this fact, some related materials (for instance, phase of stephanite,  $\text{Ag}_5\text{SbS}_4$ ) are little known from crystal-chemical and physical point of views. In order to highlight the electronic features of  $\text{Ag}_5\text{SbS}_4$ , we present here some modern NQR data concerning this compound and comparative analysis in the context of associated materials, such as stibnite (antimonite)  $\text{Sb}_2\text{S}_3$  and pyrargyrite  $\text{Ag}_3\text{SbS}_3$ .

#### 4.1 Crystal-chemistry of $\text{Sb}_2\text{S}_3$ , $\text{As}_5\text{SbS}_4$ , $\text{Ag}_3\text{SbS}_3$

Stibnite ( $\text{Sb}_2\text{S}_3$ ), pyrargyrite ( $\text{Ag}_3\text{SbS}_3$ ), proustite ( $\text{Ag}_3\text{AsS}_3$ ), stephanite ( $\text{Ag}_5\text{SbS}_4$ ), and other Sb(As)-bearing sulfides and sulfosalts belong to the group of the complex chalcogenides with universal formula  $A_xB_yS_n$ , where  $A = \text{Ag}, \text{Cu}, \text{Pb}, \text{etc.}$ , and  $B = \text{As}, \text{Sb}, \text{Bi}$ . Some structural units in materials mentioned above are the same; hence the chalcogenides are rather similar. In particular, all of them consist of infinite one-dimensional chains, extended along the  $c$ -axis. One of the basic unit elements are the trigonal group  $\text{BS}_3$ , referred also to as umbrella-like complexes (Povarennykh, 1972). The differences between them, however, are substantial and are caused by different combinations of structural units, mechanisms of their connection and, of course, different kind of crystal-chemical distortions. However, these data are not always determinable with the desired accuracy by the methods of X-ray diffraction: the patterns usually obtained are averaged for all elementary cells.

The elementary cell of stephanite,  $\text{Ag}_5\text{SbS}_4$ , at room temperature corresponds to orthorhombic symmetry with the space group  $Cmc2_1$  (Fig. 4). The parameters of the unit cell are the following:  $a = 7.830 \text{ \AA}$ ,  $b = 12.450 \text{ \AA}$ ,  $c = 8.538 \text{ \AA}$  (Petrunina et al., 1970). The structure can be presented as chains formed by  $\text{SbS}_3$  complexes. These chains organize the pairs and they are oriented along the  $c$ -axis. Atoms of Ag are located between the  $\text{SbS}_3$  units of adjacent chains. According to X-ray analysis, stephanite contains a single crystal-chemical position of Sb in the structure.

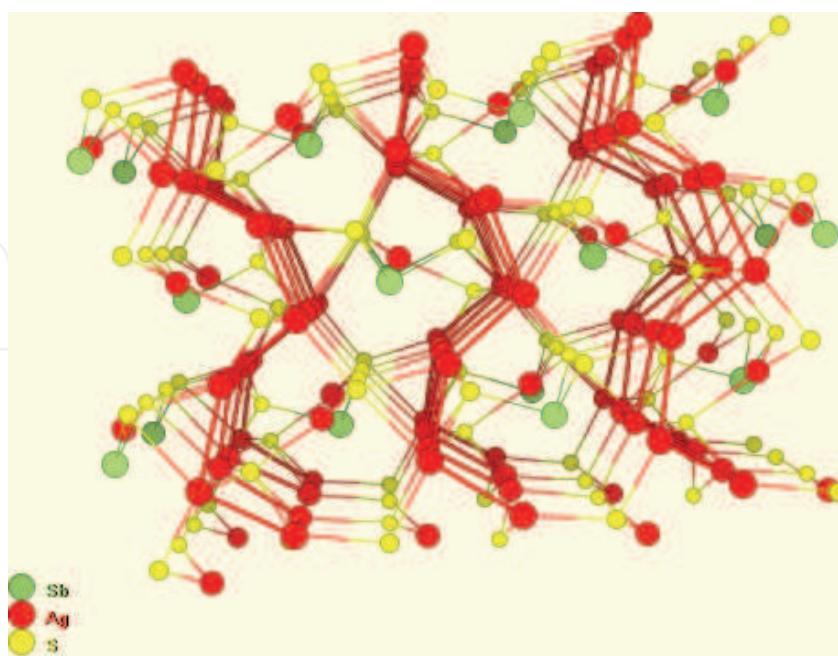


Fig. 4. Crystal structure of the stephanite,  $\text{Ag}_5\text{SbS}_4$  at room temperature. Green circles – antimony atoms, red circles – silver atoms, yellow circles – sulfur atoms.



The space group of stibnite (antimonite),  $\text{Sb}_2\text{S}_3$ , is  $Pbnm$ , the lattice constants are the following:  $a = 11.20 \text{ \AA}$ ,  $b = 11.28 \text{ \AA}$ ,  $c = 3.83 \text{ \AA}$  (Povarennykh, 1972). The lattice is constructed on the base of Sb-S-Sb zigzag-like chains, which form the double tapes  $(\text{Sb}_4\text{S}_6)_n$ . The unit cell contains two crystallographically non-equivalent Sb-positions: site *A* and site *B*.

Pyrargyrite,  $\text{Ag}_3\text{SbS}_3$ , and proustite,  $\text{Ag}_3\text{AsS}_3$ , are isostructural compounds with limited substitution between As and Sb (Povarennykh, 1972). Umbrella complexes ( $\text{BS}_3$ ) are turned by vertexes to one direction and jointed by means of Ag atoms, which form together with S atoms the helical chains elongated along the cell axis. Their space groups at room temperature are  $R3c$  with cell dimensions  $a = 10.78 \text{ \AA}$ ,  $c = 8.682 \text{ \AA}$  for proustite and  $a = 11.05 \text{ \AA}$ ,  $c = 8.74 \text{ \AA}$  for pyrargyrite. All of them have at room temperature the single crystal-chemical position of Sb(As) in the structure.

#### 4.2 NQR spectra of $\text{Sb}_2\text{S}_3$ , $\text{As}_5\text{SbS}_4$ , $\text{Ag}_3\text{SbS}_3$

In Table II the NQR frequencies of the compounds mentioned above are reported. NQR spectrum of stephanite is shown in Fig. 5. In general, it was found that antimony NQR spectra of  $\text{Sb}_2\text{S}_3$  at 77 K consist of 10 lines (Safin & Pen'kov, 1962; Abdullin et al., 1977). This fact points that stibnite have two crystallographically non-equivalent sites of antimony nuclei (Section I). Such NQR data are in good agreement with X-ray analysis studies (Section III.1), according to which there exist two antimony positions noted as site *A* and site *B*. As it should be noted from NQR spectra, *A* complexes are axially-symmetrical; asymmetry parameter of EFG tensor closes to zero ( $\eta = 0.8 \%$ ). In contrast, *B* complexes are strongly distorted ( $\eta \approx 40 \%$ ). As one can see from Table II and Fig. 5,  $^{121,123}\text{Sb}$  NQR spectra of stephanite,  $\text{Ag}_5\text{SbS}_4$ , at 77 K consist of 5 lines. This information indicates that all positions of antimony in stephanite lattice are structurally equivalent (there is a single antimony site). Non-zero value of asymmetry parameter signifies that the perceptible distortions of  $\text{SbS}_3$  pyramids take place in  $\text{Ag}_5\text{SbS}_4$ . Analogous situation happens in case of isostructural pyrargyrite,  $\text{Ag}_3\text{SbS}_3$ , and proustite,  $\text{Ag}_3\text{AsS}_3$  (Pen'kov & Safin, 1966a). For both chalcogenides, the NQR signals at 77 K are observed from one structural Sb(As) site (Table II). Analysis of NQR spectra shows that asymmetry parameters at these temperatures are not far from zero (Pen'kov & Safin, 1966a).

Material	Position	$^{121,123}\text{Sb}$ NQR frequencies, MHz ( $T = 77 \text{ K}$ )					$\eta$ , %	Ref.
		$^{121}\text{Sb}$		$^{123}\text{Sb}$				
		1/2↔3/2	3/2↔5/2	1/2↔3/2	3/2↔5/2	5/2↔7/2		
$\text{Sb}_2\text{S}_3$ (stibnite)	Site A	47.71	95.41	28.96	57.90	86.86	0.8	Safin & Pen'kov, 1962
	Site B	42.98	73.29	32.27	43.13	67.45	38.1	
$\text{Ag}_3\text{SbS}_3$ (pyrargyrite)	Single	49.84	99.70	30.28	60.52	90.78	$\approx 0$	Pen'kov & Safin, 1964
$\text{Ag}_5\text{SbS}_4$ (stephanite)	Single	54.942	108.280	34.265	65.462	98.700	10.7	This work; Pen'kov & Safin, 1966a

Table II. NQR frequencies for  $\text{Ag}_5\text{SbS}_4$  and some related compounds.

The construction of umbrella  $\text{Sb(As)S}_3$  complexes, in contrast to some complexes with transition metals (as it occurs, for example, for  $\text{CuS}_4$  units in copper chalcogenides, see Section II) suggests the presence of non-cubic local crystal fields. This circumstance shows that EFG on the Sb(As) nuclei is not caused by structural distortions (particularly, X-Sb(As)-

X angles have little changes in equitype coordination complexes  $\text{AsS}_3\text{-SbS}_3\text{-BiS}_3\text{-AsO}_3$ ). As consequence, it is obvious that  $sp$ -hybridization does not play a substantial role in creation of EFG. In this case the EFG is formed primarily due to redistribution of electronic density. It was demonstrated specially that the main factor influenced on the EFG value in NQR spectra of Sb(As)-bearing chalcogenides is a change of Sb(As)-S bond polarity (Pen'kov & Safin, 1966b), i.e. the extent of bond ionicity. Analysis of the EFG nature in a number of structural motives allows one to take into account the following aspects in distribution of electronic density: 1) ionicity-covalency of Sb(As)-S bonds, in frame of which the donor-acceptor type of bonds are also become apparent; 2) occurrence of Sb(As)-Sb(As) interactions; 3) influence of Me-S (Me is a metal element, such as Cu, Pb, Ag, and other). The donor-acceptor bonds can be realized owing to transfer of electrons from atoms-"donors", which either contains the essential number of electrons on the external  $p$ - and  $d$ -orbitals or have "unshared"  $s^2$ -electrons, to atoms-"acceptors" with the little number of electrons. Sulfur atoms (S,  $3s^23p^4$ ) can serve as donors due to both the unshared  $s^2$ -electrons and the  $p$ -electrons.

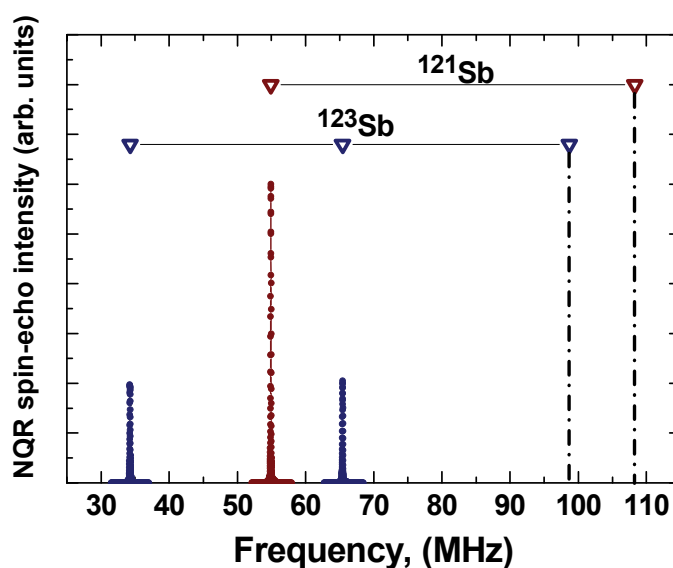


Fig. 5. Antimony NQR spectra for  $\text{Ag}_5\text{SbS}$ . Triangular symbols point to the positions of  $^{121,123}\text{Sb}$  NQR signals. The vertical dashed lines point to the positions of two Sb NQR signals, which were not studied. For details, see text.

In this context, let us discuss at first the EFG origin in stibnite,  $\text{Sb}_2\text{S}_3$  (Safin & Pen'kov, 1962; Abdullin et al., 1977). Interestingly, the values of NQR frequencies for antimony in  $B$  site are notably less than NQR frequencies for this element in  $A$  site. As it was proposed, Sb-S bonds in case of  $B$  site appear to be more covalent as compared with bonds, corresponding to  $A$  site. The increasing of covalent effect is explained by manifestation of additional bonds, having the donor-acceptor nature. These contacts should decrease the value of effective charge on the antimony atom. Taking into account these aspects, the coordination number of Sb atoms located in  $B$  position increases up to 5. Corresponding coordination polyhedron can be visualized as a distorted semi-octahedron  $\text{SbS}_5$ .

In case of "metallic" chalcogenides situation is more complex. In contrast to binary Sb(As)-bearing compounds, the crystal electric fields, caused by Sb(As)-S bonds in frame of  $\text{SbS}_3(\text{SbS}_5)$  complexes, are influenced also by the fields created by metallic atoms (Cu, Ag



and other). These interactions lead to appearance of twofold consequence. First factor is a so-called steric effect: Sb(As) and S atoms are repulsed. Second factor is an induction effect, according to which the metallic atoms “remove” part of electronic density. These effects are closely associated and usually coexist. As a result, Sb(As)-S bonds are “loosened” and they become more polar. This leads, as a rule, to increase of NQR frequencies. The pyrrargyrite-proustite phases  $\text{Ag}_3[\text{Sb}(\text{As})]\text{S}_3$  may serve as an excellent example of such behavior (Pen'kov & Safin, 1966a). As it was found, the natural samples of pyrrargyrite,  $\text{Ag}_3\text{SbS}_3$ , can contain a little number of As impurity; these substitution atoms occupy the positions of Sb. The resonance frequency shift for As impurities indicates the existence of more ionic nature for the As-S bonds in  $\text{Ag}_3\text{SbS}_3$  matrix than for those in the etalon samples of proustite,  $\text{Ag}_3\text{AsS}_3$ . The increasing of ionicity is explained by steric inconsistency: actually, the covalent radiuses of As and Sb atoms are 1.21 and 1.41 Å, respectively. In this case, the impurity atoms are forced to accommodate themselves into the structural positions and dimensions of “native” matrix atoms.

Now, it is easier to discuss the EFG nature in stephanite,  $\text{Ag}_5\text{SbS}_4$ . Indeed,  $^{121,123}\text{Sb}$  NQR frequencies for  $\text{Ag}_5\text{SbS}_4$  are higher than that for binary stibnite,  $\text{Sb}_2\text{S}_3$ . This fact provides evidence that the “metallic” twofold factor, in addition to “standard” donor-acceptor bonds, also exists in  $\text{Ag}_5\text{SbS}_4$ . Moreover, the values of NQR frequencies for  $\text{Ag}_5\text{SbS}_4$  exceed the values of resonance frequencies exhibited by pyrrargyrite,  $\text{Ag}_3\text{SbS}_3$ . Therefore, Sb-S bonds in stephanite appear to be more polar than in stibnite and pyrrargyrite. This circumstance implies also that the higher NQR frequencies (as compared with pyrrargyrite) are associated with a higher coordination number of the Ag atoms (in other words, with stronger induction interaction of the Sb-S and Ag-S bonds).

#### 4.3 Temperature dependences of NQR spectra of $\text{Sb}_2\text{S}_3$ , $\text{As}_5\text{SbS}_4$ , $\text{Ag}_3\text{SbS}_3$

The study of spectroscopic parameters (NQR frequencies,  $\nu_Q$ , NQR line-widths,  $\Delta\nu_Q$ , and asymmetry parameter,  $\eta$ ) as a function of temperature ( $T$ ) immediately provides important information since the components of EFG tensor are very sensitive to small atomic displacements or modifications of charge distribution.

Let us describe at first the recent data for stephanite phase,  $\text{Ag}_5\text{SbS}_4$ . As it was noted above,  $^{121,123}\text{Sb}$  NQR spectrum of  $\text{Ag}_5\text{SbS}_4$  at  $T = 77$  K consists of five lines (Fig. 5). It is quite enough to observe only three of five NQR lines in order to detect any possible anomalies in temperature dependences of spectroscopic characteristics and calculate asymmetry parameter,  $\eta$  (Section I). In general, we studied the temperature dependences (4.2–300 K) of the following resonance frequencies and their line-widths:  $\nu_{Q1}(\pm 1/2 \leftrightarrow \pm 3/2)$ ,  $\nu_{Q2}(\pm 3/2 \leftrightarrow \pm 5/2)$  for  $^{123}\text{Sb}$ , and  $\nu_{Q3}(\pm 1/2 \leftrightarrow \pm 3/2)$  for  $^{121}\text{Sb}$ . The Sb NQR line shapes were well fitted by Lorentzian function at all temperatures studied (corresponding line-widths were taken as a full width at half maximum). The temperature dependence of  $\nu_{Q1}$  is presented in Fig. 6.

On the whole, the quadrupole frequency  $\nu_{Q1}$  decreases with increasing temperature without any significant anomalies. Thus, it is possible to exclude the major structural transitions. At the same time, we point out on the weak change in the slope of the  $\nu_{Q1}$  versus  $T$  dependence at about 145 K. The temperature dependences of line-widths  $\Delta\nu_{Q1}$  and  $\Delta\nu_{Q2}$  are displayed in Fig. 7. It is important that the line-widths at all temperatures studied are not larger than 90 kHz. Such values, taking into account the stephanite complexity, imply this compound represents a high-ordered structure. As one can see, the NQR line-widths decrease rather weakly with decreasing of temperature in the range of 4.2–145 K, but it seems that one of the lines ( $\Delta\nu_{Q2}$ ) narrows more drastically above 145 K.

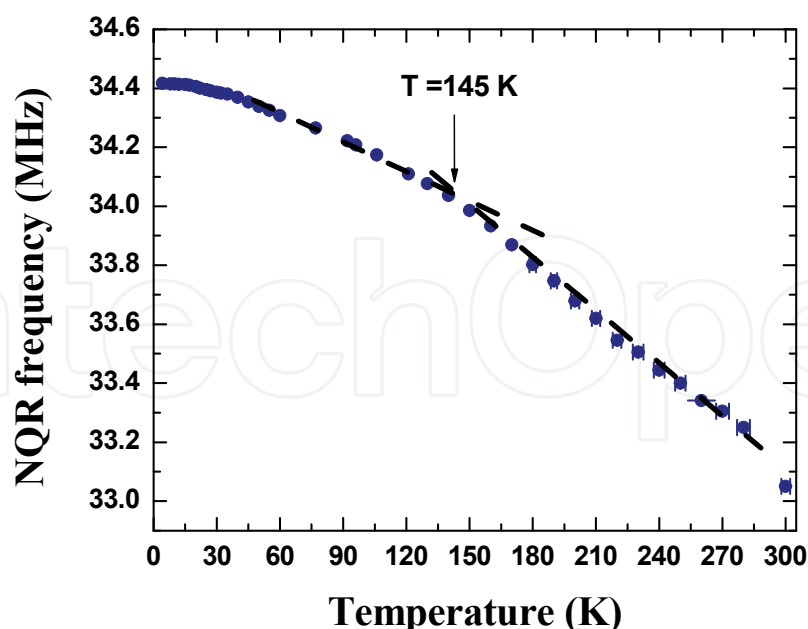


Fig. 6. The temperature dependence of  $^{123}\text{Sb}$  NQR frequency  $\nu_{Q1}$  (transition  $\pm 1/2 \leftrightarrow \pm 3/2$ ) for  $\text{Ag}_5\text{SbS}_4$ . Arrow points to the positions of the change of slope in the  $\nu_{Q1}(T)$  dependence at 145 K, curves are guides for eyes. For details, see text.

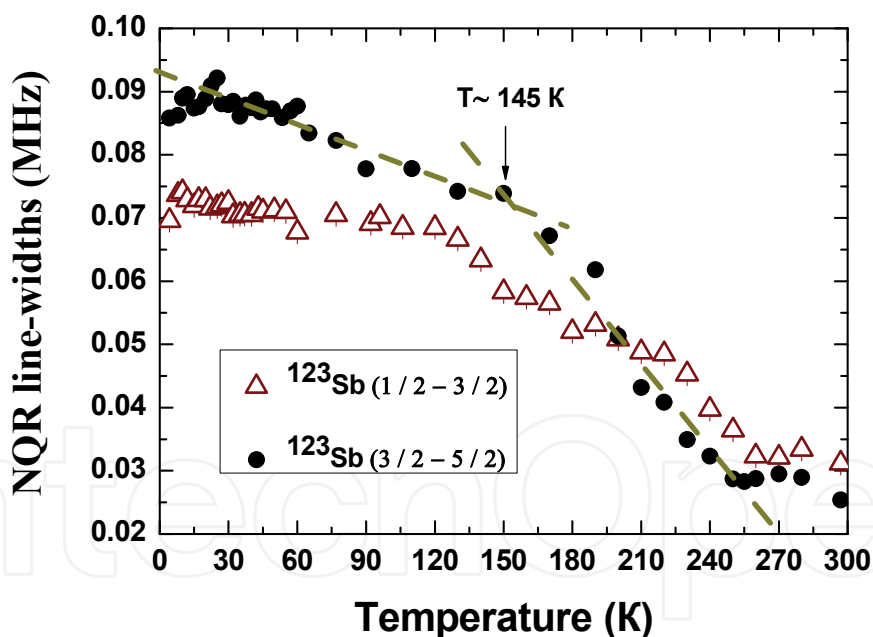


Fig. 7. The temperature dependence of  $^{123}\text{Sb}$  NQR line-widths  $\Delta\nu_{Q1}$  (transition  $\pm 1/2 \leftrightarrow \pm 3/2$ ) and  $\Delta\nu_{Q2}$  (transition  $\pm 3/2 \leftrightarrow \pm 5/2$ ) for  $\text{Ag}_5\text{SbS}_4$ . Arrow points to the positions of the change of slope in the  $\Delta\nu_{Q2}(T)$  dependence at 145 K, curves are guides for eyes. For details, see text.

More accuracy and detailed information can be extracted on the base of temperature dependence of asymmetry parameter (Fig. 8). In general, the value of  $\eta$  changes in frame of a small range (in the vicinity of 10 %). This aspect indicates about noticeable, but not large distortions of umbrella  $\text{SbS}_3$  complexes, which can be interpreted in character as deviation of the local symmetry for  $\text{SbS}_3$  unit from the axial one. More exciting aspect is an intelligible

bend, which takes place at 145 K. Such changes in spectroscopic characteristics (in our case about 145 K) represent the characteristic features of phase transitions (Grechishkin, 1973). The lack of NQR frequency jumps and/or changes of number of lines in NQR spectrum prove the absence of dramatic structural transformations near 145 K.

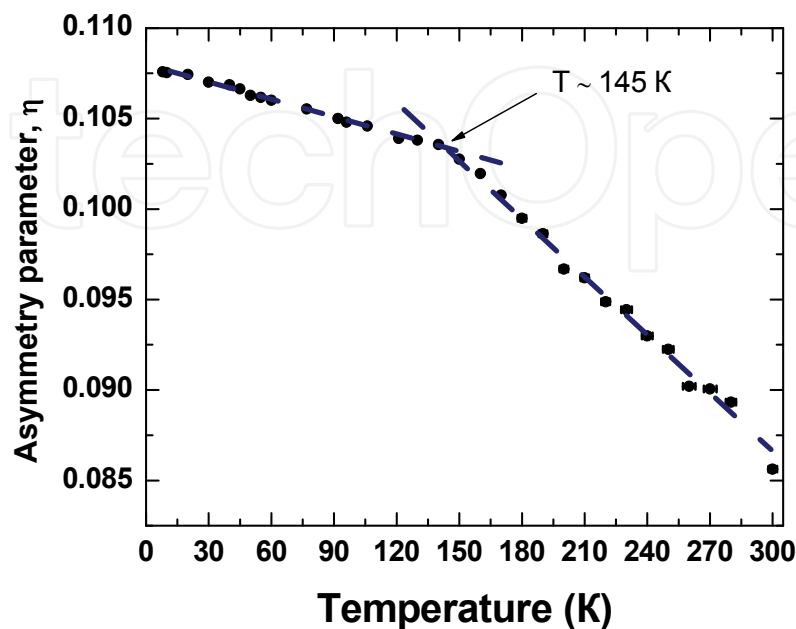


Fig. 8. The temperature dependence of asymmetry parameter,  $\eta$ , for  $\text{Ag}_5\text{SbS}_4$ . Arrow points to the positions of the change of slope in this dependence at 145 K, curves are guides for eyes. For details, see text.

Let us compare the NQR features that characterize the phase transition in stephanite,  $\text{Ag}_5\text{SbS}_4$  with those for stibnite,  $\text{Sb}_2\text{S}_3$ , and pyrargyrite-proustite series,  $\text{Ag}_3[\text{Sb}(\text{As})]\text{S}_3$  (more detailed analysis will be presented in forthcoming paper). Actually, both the stibnite and the pyrargyrite-proustite have the ferroelectric properties, but these properties become apparent by different ways. In particular, it is known that the single  $^{75}\text{As}$  NQR line for proustite,  $\text{Ag}_3\text{AsS}_3$ , at  $T > 60$  K and  $T < 24$  K splits into 8 lines at least, in spite of the fact that no structural transformation in this critical region was found by X-ray diffraction investigation (Bondar' et al., 1983). Analysis of NQR data shows that such anomalies can be understood in terms of existence in crystal under study of so-called incommensurate phase, which is caused by interacting oscillating modes of the crystal (modern data can be found, for instance, in (Apih et al., 2000)). Notably, similar splitting was observed also in case of  $^{121,123}\text{Sb}$  NQR lines for pyrargyrite phase,  $\text{Ag}_3\text{SbS}_3$ , (Baisa et al., 1977). Obviously, stephanite sample,  $\text{Ag}_5\text{SbS}_4$ , related to pyrargyrite-proustite series from crystal-chemical point of view does not follow the similar mechanism. Instead of this, NQR measurements on single antimony site in  $\text{Ag}_5\text{SbS}_4$  resemble in some extent the NQR studies performed on both antimony sites (*A* and *B*) in stibnite,  $\text{Sb}_2\text{S}_3$  (Abdullin et al., 1977). Indeed, there is no any splitting of NQR lines, but a number of weak anomalies were observed at 140, 225,  $\approx 300$ , 355, and 420 K. As it was found, these anomalies correspond to phase transitions of second order, which are accompanied by slight structural reorganizations of antimony coordination spheres, leading to transformations of ferroelectric properties. It seems that stephanite,  $\text{Ag}_5\text{SbS}_4$ , and stibnite,  $\text{Sb}_2\text{S}_3$ , have several common features in lattice dynamics that emphasize in some extent their relationship in electronic properties. In this context, our NQR results can be considered as the probing studies and, simultaneously, as a basis for further studies  $\text{Ag}_5\text{SbS}_4$  with application of more specific methods.

## 5. Conclusions

Our examples of NQR spectroscopic studies of copper, antimony, and arsenic chalcogenides show that rather broad and diverse information may be obtained. There are themes typical to many solid state investigations, i.e. phase transitions, the relation of electric field gradients to electronic structure. NQR has proven to be an indispensable tool in this field.

## 6. Acknowledgment

This work is partly supported by the Grant RNP-2.1.1/6183 from the Ministry of Education and Science, Russian Federation.

## 7. References

- Abdullin, R.S.; Pen'kov, I.N.; Nizamutdinov, N.M.; Grigas, I. & Safin, I.A. (1977). Temperature dependence of NQR spectra of  $^{121,123}\text{Sb}$  in  $\text{Sb}_2\text{S}_3$ . *Physics of the Solid State*, 19, 1632-1635.
- Abdullin, R.S.; Kal'chev, V.P.; Pen'kov, I.N. (1987). Investigation of copper minerals by NQR: crystallochemistry, electronic structure, lattice dynamics. *Phys. Chem. Minerals*, 14, 258-263.
- Abrikosov, N.K.; Bankina, V.F.; Poretskaya, L.V.; Skudnova, E.V. & Chizhevskaya, S.N. (1975). *Semiconducting chalcogenides and their alloys*, Publishing House Nauka, Moscow.
- Anashkin, V.N.; Kalinina, T.A.; Matukhin, V.L.; Pen'kov, I.N. & Safin, I.A. (1994). NQR spectra of  $^{63,65}\text{Cu}$  in coexisting covellite ( $\text{CuS}$ ) and geerite ( $\text{Cu}_{1,6}\text{S}$ ). *Proceedings Rus. Mineral. Soc.*, 5, 59-63.
- Apih, T.; Mikac, U.; Dolinšek, J.; Seliger, J. & Blinc, R. (2000). Unique 1- $q$  and 3- $q$  incommensurate phases in proustite:  $^{75}\text{As}$  NQR line-shape and spin-lattice relaxation study. *Phys. Rev. B*, 61, 1003-1013.
- Baisa, D.F.; Bondar', A.V. & Gordon, A.Ja. (1977). The phase transition "order-disorder" in pyrrargyrite. *Physics of the Solid State*, 19, 1273-1276.
- Berry, L.G. (1954). The crystal structure of covellite,  $\text{CuS}$ , and klockmanite,  $\text{CuSe}$ . *Am. Mineral.*, 39, 504-509.
- Blinc, R. & Zeks, B. (1974). *Soft modes in ferroelectrics and antiferroelectrics*, Elsevier, New York.
- Bondar', A. V.; Vihnin, V. S.; Rjabchenko, S. M. & Jachmenov, V. E. (1983). Incommensurate phase near the second-order phase transition in proustite. *Physics of the Solid State*, 25, 2602-2609.
- Buckel, W. & Hilsch, R. (1950). Zur Supraleitung von Kupfersulfid. *Z. für Physik*, 128, 324-346.
- Di Benedetto, F.; Borgheresi, M.; Caneschi, A.; Chastanet, G.; Cipriani, C.; Gatteschi, D.; Pratesi, G.; Romanelli, M. & Sessoli R. (2006). First evidence of natural superconductivity. *Eur. J. Mineral.*, 18, 283-287.
- Evans, H. T. Jr. & Konnert, J. A. (1976). Crystal structure refinement of covellite. *Am. Mineral.*, 61, 996-1000.
- Fjellvåg, H.; Grønvold, F.; Stølen, S.; Andresen, A.F.; Müller-Käfer, R. & Simon, A. (1988). Low-temperature structural distortion in  $\text{CuS}$ . *Z. für Kristallogr.*, 184, 111-121.
- Gainov, R. R.; Dooglav, A. V.; Pen'kov, I. N.; Mukhamedshin, I. R.; Mozgova, N. N.; Evlampiev, I. A. & Bryzgalov, I. A. (2009). Phase transition and anomalous electronic behavior in the layered superconductor  $\text{CuS}$  probed by NQR. *Phys. Rev. B.*, 79, 075115.
- Grechishkin, V.S. (1973). *Nuclear quadrupole interactions in solids*, Nauka (in Russian), Moscow.

- Goble, R.J. (1985). The relationship between crystal structure, bonding and cell dimensions in the copper sulfides. *Can. Mineral.*, 23, 61-76.
- Gablina, I.F. (1997). Copper sulfides as indicators of the ore-forming environment. *Transactions RAS.* 357, 1133-1137.
- Izoitko, V.M. (1997). *Technological mineralogy and estimation of ore*, Nauka, St. Petersburg.
- Isac, L.A.; Duta, A.; Kriza, A.; Enesca, I.A. & Nanu, M. (2007). The growth of CuS thin films by Spray Pyrolysis. *J. Phys.: Confer. Series*, 61, 477-481.
- Itoh, Y.; Hayashi, A.; Yamagata, H.; Matsumura, M.; Koga, K. & Ueda, Y. (1996). Cu NMR and NQR study of CuS. *J Phys Soc Japan (letters)*, 65, 1953-1956.
- Kaufmann, E.N. & Vianden, R.J. (1979). The electric field gradient in non-cubic metals. *Rev. Mod. Phys.*, 51, 161-214.
- Meissner, W. (1929). Messungen mit Hilfe von flüssigem Helium. V. Supraleitfähigkeit von Kupfersulfid. *Z. für Physik*, 58, 570-572.
- Milman, V. (2002). Klockmannite, CuSe: structure, properties and phase stability from ab initio modeling. *Acta Cryst. B.*, 58, 437-447.
- Nozaki, H.; Shibata, K.; Ishii, M. & Yukino, K. (1995). Phase transition of CuS<sub>1-x</sub>Se<sub>x</sub> (0≤x≤1) studied by X-ray diffractometry. *J. Solid State Chem.*, 118, 176-179.
- Ohmasa, M. ; Suzuki, M. & Takeuchi, Y. (1977). A refinement of the crystal structure of covellite, CuS. *Mineral. J. (Japan)*, 8, 311-319.
- Peiris, S.M.; Pearson, T.T. & Heinz, D.L. (1998). Compression of klockmannite, CuSe. *J. Chem. Phys.*, 109, 634-636.
- Pen'kov, I.N. & Safin, I. A. (1964). Nuclear quadrupole resonance in proustite and pyrargyrite. *Physics of the Solid State*, 6, 2467-2470.
- Pen'kov, I.N. & Safin, I. A. (1966a). NQR study of stephanite (Ag<sub>5</sub>SbS<sub>4</sub>). *Dokl. Akad. Nauk SSSR*, 168, 1148-1150.
- Pen'kov, I.N. & Safin, I. A. (1966b). Application of nuclear quadrupole resonance in study of minerals. *Izv. Akad. Nauk SSSR (Geol. Ser)*, 12, 41-52.
- Petrunina, A.A.; Maksimov, B.M. & Iljuhin, V.V. (1970). Crystal Structure of Stephanite Ag<sub>5</sub>SbS<sub>4</sub>. *Sov. Phys. Dokl.*, 188, 342-346.
- Povarennykh, A.S. (1972). *Crystal chemical classification of minerals*, Plenum Press, New York.
- Rigamonti, A.; Borsa, F. & Carretta, P. (1998). Basic aspects and main results of NMR-NQR spectroscopies in high-temperature superconductors. *Rep. Prog. Phys.*, 61, 1367-1439.
- Safin, I. A. & Pen'kov, I.N. (1962). NQR in stibnite. *Dokl. Akad. Nauk SSSR*, 147, 2, 410-413.
- Saito, S.-H.; Kishi, H.; Nie, K.; Nakamaru, H.; Wagatsuma, F. & Shinohara, T. (1997). <sup>63</sup>Cu NMR studies of copper sulfide., *Phys. Rev. B* 55, 14527-14535.
- Sampathkumaran, E.V.; Gupta, L.C. & Vijayaraghavan, R. (1979). Valence fluctuation and the temperature dependence of copper nuclear quadrupole interaction in EuCu<sub>2</sub>Si<sub>2</sub> and YbCu<sub>2</sub>Si<sub>2</sub>. *Phys. Rev. Lett.*, 43, 1189-1192.
- Semin, G.K.; Babushkina, T.A. & Yakobson, G.G. (1975). *Nuclear quadrupole resonance in chemistry*, John Wiley & Sons, New York.
- Slichter, C.P. (1996). *Principles of magnetic resonance (3<sup>rd</sup> enriched and updated edition)*, Springer-Verlag, Berlin.
- Torumba, D.; Parlinski, K.; Rots, M. & Cottenier, S. (2006). Temperature dependence of the electric-field gradient in hcp-Cd from first principles. *Phys. Rev. B.*, 74, 144304.
- Wilson, J.A. (2009). A perspective on the pnictide superconductors. Cornell University Library (<http://arxiv.org/abs/0809.0560>)





## **Superconductor**

Edited by Doctor Adir Moyses Luiz

ISBN 978-953-307-107-7

Hard cover, 344 pages

**Publisher** Sciyo

**Published online** 18, August, 2010

**Published in print edition** August, 2010

This book contains a collection of works intended to study theoretical and experimental aspects of superconductivity. Here you will find interesting reports on low- $T_c$  superconductors (materials with  $T_c < 30$  K), as well as a great number of researches on high- $T_c$  superconductors (materials with  $T_c > 30$  K). Certainly this book will be useful to encourage further experimental and theoretical researches in superconducting materials.

### **How to reference**

In order to correctly reference this scholarly work, feel free to copy and paste the following:

R.R. Gainov, A.V. Dooglav, I.N. Penkov, A.Yu. Orlova, I.A. Evlampiev, N.N. Mozgova and R.R. Khasanov (2010). Determination of the Local Crystal-Chemical Features of Complex Chalcogenides by Copper, Antimony, and Arsenic NQR, Superconductor, Doctor Adir Moyses Luiz (Ed.), ISBN: 978-953-307-107-7, InTech, Available from: <http://www.intechopen.com/books/superconductor/determination-of-the-local-crystal-chemical-features-of-complex-chalcogenides-by-copper-antimony-and>

**INTECH**  
open science | open minds

### **InTech Europe**

University Campus STeP Ri  
Slavka Krautzeka 83/A  
51000 Rijeka, Croatia  
Phone: +385 (51) 770 447  
Fax: +385 (51) 686 166  
[www.intechopen.com](http://www.intechopen.com)

### **InTech China**

Unit 405, Office Block, Hotel Equatorial Shanghai  
No.65, Yan An Road (West), Shanghai, 200040, China  
中国上海市延安西路65号上海国际贵都大饭店办公楼405单元  
Phone: +86-21-62489820  
Fax: +86-21-62489821



© 2010 The Author(s). Licensee IntechOpen. This chapter is distributed under the terms of the [Creative Commons Attribution-NonCommercial-ShareAlike-3.0 License](https://creativecommons.org/licenses/by-nc-sa/3.0/), which permits use, distribution and reproduction for non-commercial purposes, provided the original is properly cited and derivative works building on this content are distributed under the same license.

IntechOpen

IntechOpen